Available online at sjuoz.uoz.edu.krd

Science Journal of University of Zakho

Vol. 11, No. 3, pp. 427– 439, July-September, 2023

p-ISSN: 2663-628X
e-ISSN: 2663-6298

BIOSYNTHESIS AND CHARACTERIZATION OF CuO NANOPARTICLES FROM FERULAGO ANGULATE LEAF EXTRACT USING DIFFERENT pH

Saniya Sadullah Omar[a*], Raghad Y. Mohammed[b]

College of Science, University of Duhok, Kurdistan Region, Iraq - (saniya.saadullah@gmail.com, ssraghad@uod.ac)

Received: 30 Jan., 2023 / Accepted: 14 May, 2023 / Published: 21 Aug. 2023 *https://doi.org/10.25271/sjuoz.2023.11.3.1112*

ABSTRACT

CuO nanoparticles are synthesized from Ferulago angulate leaf extract under different pH values. The structural, morphological, as well as optical properties of the green synthesized CuO NPs are studied. Besides, the functional groups in the Ferulago angulate stabilizer capping the copper nanoparticles were examined using FTIR spectra. The primary factor that led to the first confirmation of CuO NP production was the reaction mixture's color change. A phytochemical test revealed the presence of proteins, amino acids, carbohydrates, flavonoids, phenols, alkaloids, tannins, and saponins. FTIR spectrum shows a peak at 532.35 cm^{-1}, this may be attributed to CuO's vibrations confirming the presence of copper oxide nanoparticles. XRD analysis shows the presence of crystalline monoclinic cupric oxide (CuO). The morphological study (FESEM) shows different morphology (different shapes and sizes) under different pH values. EDS data shows the O-richness of the prepared CuO NPs extracted from Ferulago angulate [Schltdl.] BOISS leaf extract shows pure CuO phases. In this investigation, fabricated CuO's estimated energy band gap values were higher than those of bulk CuO. Results show Eg increment with increasing pH values.

KEYWORDS: Green synthesis, CuO NPs, Ferulago Angulate [Schltdl.] BOISS, Phytochemical Screening, Characterization.

1. INTRODUCTION

Modern materials science includes an important field known as nanotechnology. It is involved in the fabrication and development of many nanoparticles with sizes ranging from 1 to 100 nm. In modern research, nanotechnology plays an important role, including applications in pharmacy, health, biomedical sciences (Bukhari *et al.,* 2021), electronics, food, pharmaceuticals (Peddi *et al.,* 2021), chemistry, the chemical industry, cosmetics, and the energy sciences, mechanics, space technology, and environmental health, (Hassan et al., 2019). Due to their potential as a cheap alternative instead of costly noble metals nanoparticles are used as catalysts in many industrial chemical processes. Lots of interest has been paid to the fabrication of nanoparticles from inexpensive and plentiful metals found on Earth (Shamsuddin & Raja Nordin, 2019).

As the bulk material scale decreases to the nanoscale, its physicochemical properties change. The optical, electrical, and magnetic properties of nanosized particles differ from those of the same material's bulk version.(Thamer *et al.*, 2018).

Metal nanoparticles have many applications due to their unique optical, electrical, mechanical, magnetic, and chemical properties. Nanoparticles have been produced via chemical, physical and biological methods. Even though the majority of approaches produce nanoparticles that are clean and well-defined, these approaches are either very expensive or have the potential to be harmful to the natural environment (Altikatoglu *et al*., 2017).

Copper oxide nanoparticles (CuO NPs) are a type of semiconducting material (Rehman et al., 2022) that has recently been gaining lots of interest due to their unique electrical, optical, and catalytic properties. They have been used in lithium-ion electrode materials, sensors, photovoltaic devices, catalysis, biomedicine, and so on (Manasa et al., 2021).

CuO is a p-type semiconductor material that has a direct bulk bandgap of 1.2 eV and a refractive index of 2.63 (Horti et al., 2020). It has the space group C2/c and crystallizes in the monoclinic phase (No. 15). CuO-NPs are widely used in gas sensors, batteries, biosensors, giant magnetoresistance materials, catalysts, superconductors, solar cells (Taran *et al.*, 2021), high-temperature superconductors magnetic storage media, catalysis (Gawande *et al.*, 2016), (Kwak & Kim, 2005), and photocatalysis for water purification environment (Sone *et al.*, 2020). The sol-gel approach (Othman *et al.*, 2013), microwave irradiations (Elazab, 2018), thermal decomposition (Salavati-Niasari & Davar, 2009), an electrochemical method (Velusamy *et al.*, 2018), and an alkoxide-supported technique have also been utilized in the fabrication of CuO-NPs (Grigore *et al.*, 2016).

Even though most approaches produce clean, well-defined nanoparticles, they are either costly or harmful to the environment. Moreover, due to the use of toxic substances, high contaminants, and excessive energy consumption in produced NPs, these approaches have been drawn while biosynthesized CuO-NPs are considered a safe fabrication method. Especially in medical applications, the use of gregarious and single cells microorganisms such as actinomycetes, fungi, bacterium, plants, or algal during the green CuO-NPs synthesis is preferred (Hassan et al., 2019).

Recently systems are extensively spread along co-logical boundaries (Rehman et al., 2022)

making them conveniently accessible and well-controlled. The utilization of physical and chemical techniques has significantly decreased due to the green products of nanoparticles (Shanan *et al.*, 2018). The CuO nanoparticles in this research study were produced by an environmentally friendly process known as green synthesis.

The fabricated CuO nanoparticles were characterized using a variety of characterization methods including Fourier transform infrared spectroscopy (FTIR), X-ray diffraction diffractometer

* Corresponding author

(XRD), Field Emission Scanning Electron Microscope (FESEM, and UV-visible spectroscopy.

2. MATERIALS AND METHODS

2.1 Materials Required:

Copper (II) nitrate trihydrate Cu $(NO_3)_2.3H_2O$ and sodium hydroxide (NaOH) was purchased from Sigma Aldrich Company and used as received.

2.2 Preparation of Ferulago ANGULATE [Schltdl.] BOISS Leaf extracT:

Fresh Leaves of *Ferulago angulate [Schltdl.]* BOISS (Figure 1a) was collected in April 2021 from Gara Mountain in the Kurdistan region- of Iraq. To remove any dirt particles, the leaves were washed and rinsed 3 times with distilled water, then dried in the shadow at room temperature for one month. Using a 500 W combined grinder, the dried leaves were ground into powder. Then 50 g of dried *ferulago angulata* leaf powder contained in 500 ml of distilled water was boiled at 70 C° for 20 minutes.
Afterward, the solution was gradually cool down to reach room temperature. It should be noted that after the boiling process, the color of the solution changed to light orange color (Figure 1 b).

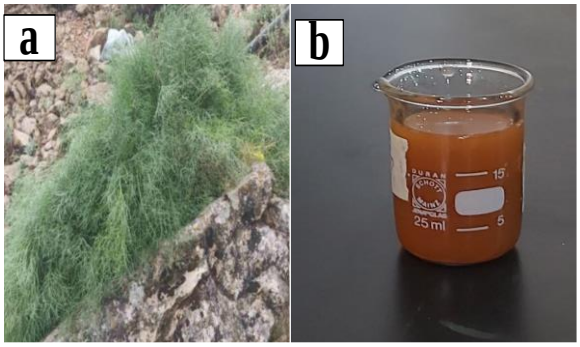

Figure 1: (a) Ferulago angulate [Schltdl.] BOISS fresh Leaf and, (b): Ferulago angulate [Schltdl.] BOISS extract.
Afterward, the solution mixture was filtered using Whatman filter paper No. 2 paper, and then the filtrate was concentrated by rotary evaporation for 15 minutes at room temperature. Then the extract was stored at 4°C for the synthesis of copper oxide nanoparticles.

2.3Phytochemical tests of Ferulago angulate [Schltdl.] BOISS Leaf extracT:

As shown in Figure 2, the plant extracts were tested for preliminary phytochemical screening.

Flavonoid test:
Concentrate H_2SO_4 test
The presence of flavonoids was shown by the production of an orange color after a few drops of concentration H_2SO_4 was added to 1 ml of extraction (Nafeesa et al, 2017) (Tyagi, 2017).
Lead acetate test:
To 1 ml of each extract, a few drops of a lead acetate solution containing 10% were added. The yellow precipitate indicates flavonoids (Singh & Kumar, 2017).
Carbohydrate test:
Molish's test (general test)
A test tube was filled with 1 ml of extract, and 5 drops of alcoholic α—naphthol, and was vigorously shaken before 1 ml of concentrated H_2SO_4 was slowly added to the tube wall to create a violet ring. This proved that there were carbs present (Lakshmibai et al., 2015) (Sivaranjani, 2021).
Alkaloid test:
Wagner's test:
Each extract was acidified and given 2 Wagner's reagent drops (1.25gm of iodine with 2gm KI and distilled water to create a final size of 100ml). Alkaloids are present when brown and reddish precipitate forms along the test tube's sides (Kardong *et al.*, 2013).
Tannin test:
Ferric chloride test:
Braymer's testing for tannins involves placing 1 ml of each extract in a test tube, adding 3 ml of distilled water, boiling it, and then adding 1 ml of 1% ferric chloride. If blue-green, brownish-green, or bluish-black stains develop, tannins are present. (Uma et al., 2017)(Kardong et al., 2013)(Giri et al., 2016)
Saponin test:
Foam test:
A little quantity of extract should be dissolved in 3ml of distilled water after being forcefully shaken and left for 1 minute, semi-permanent substances, such as foam, can detect saponins (Banso, 2009).
Aqueous mercury chloride (Hg_2Cl_2) test:
Aqueous mercury chloride was used as a reagent in the saponin test, which used (5%) aqueous mercury chloride. Each extract and the reagent were mixed in a1 ml of distilled water. The formation of a white precipitate is a sign that saponin is present (Harborne, 1973).
Proteins and amino acid test:
Ninhydrin test (free amino acid test)
After adding 1 ml of the 1% ninhydrin reagent to the extract and heating it for 10 minutes in a water bath, the color of the amino acids (purple) was revealed (Melkamu & Bitew, 2021).
Proteins test (Biuret test)
2 ml of extract were combined with 5 drops of copper sulfate solution, 1 ml of ethanol, and then pellets of potassium hydroxide. The ethanolic layer became pink, indicating the presence of peptide bonds (Tyagi, 2017).
Phenolic test:
Lead acetate test
A white phenol precipitate was created by mixing 5 ml of distilled water with 1 ml of each extract and 3 ml of 10 % lead acetate (Naik & Sellappan, 2019), (Kardong et al., 2013).
Ferric chloride test:
Adding a few drops of a 5 percent solution of ferric chloride to 1 ml of each extract. The existence of phenols was indicated by blue-black or dark green color (Naik & Sellappan, 2019).

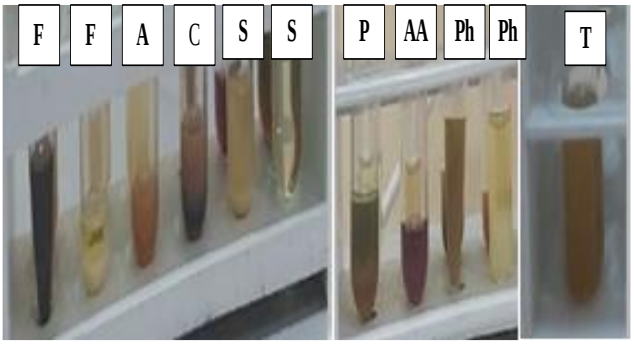

Figure 2: Phytochemical Test of Ferulago angulate [Schltdl.] BOISS Leaf extract. F: Flavonoid, A: Alkolid, C: Carbohydrate, S: Saponin, P: Protein, AA: Amino Acid, Ph: Phenol, T: Tannin.

Ferulago angulata, (Schlecht.) Boiss., also known as "Chavil" or "Chavir" in Persian, is described in the literature as a folk medicine, a food additive, particularly when used with dairy products, and an aromatic plant that is produced in the Kurdistan region of Iraq (Fig 3). The aerial parts of Ferulago angulata have shown in previous phytochemical screening studies for bioactive compounds to be a rich source of flavonoids, phenols, coumarins

such as pyranocoumarins and furanocoumarins, monoterpene hydrocarbons such as α-Pinene, myrcene, α-Phellandrene, trans-β-Ocimene, oxygenated monoterpenes such as thymol, sesquiterpenes, and sesquiterpene lactones(Jiménez et al., 2000)(Mabry & Moubasher, 1990)(Doganca et al., 1991)(Khalighi-Sigaroodi et al., 2006)(M. Naseri, 2013)(Javidnia & Khoshneviszadeh, 2006). Moreover, findings from ethnobotanical studies showed that *Ferulago angulata* is used as a medicine for headaches, spleen, and snake bites (Monfared et al., 2006)(Shahabi et al., 2007), in addition to being an anti-diabetic, tonic, sedative, aphrodisiac, and anti-hemorrhoids (Hosseini et al., 2012). Our results are in agreement with many research groups(Hosseini et al., 2012)(Azarbani et al., 2014)(Golfakhrabadi et al., 2016)(Karimian et al., 2014), who confirmed the presence of phenolic and flavonoid compounds, tannins, alkaloids, carbohydrates, saponin, amino acids, and proteins as shown in Fig.2 as these aromatic compounds contain hydroxyl groups that are adjacent to an aromatic ring can play an important role as capping and reducing agent for CuO-NPs

α- Pinene Myrcene

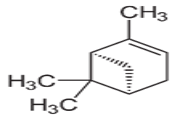

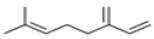

Hesperetin Xanthotoxin

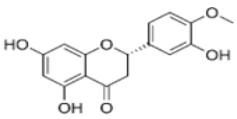

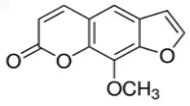

Isoimperatorin

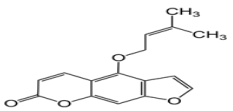

Oxypeucedanin β-sitosterol linoleate

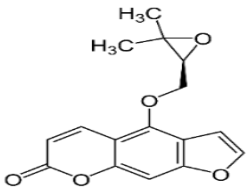

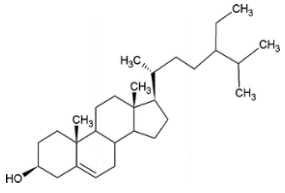

Figure 3: Ferulago angulate (picture of the author) and chemical structures of common secondary metabolites.

2.4 PREPARATION OF COPPER OXIDE NANOPARTICLES:

CuO nanoparticles were synthesized by reducing copper (II) nitrate trihydrate (Cu(NO3)2.3H2O), using fresh leaves extracted from the Ferulago angulate plant (Kiflom Gebremedhn *et al.*, 2019).

1 ml of Cu $(NO_3)_2.3H_2O$ was dissolved in 50 ml of distilled water and then the solution was magnetically stirred for 5 minutes at room temperature. To synthesize CuO NPs, 1M sodium hydroxide (NaOH) was added to 20 ml of distilled water and stirred magnetically for 15 minutes at room temperature.

After combining the two solutions, 25 ml of Ferulago Angulate (Schltdl.) BOISS leaves extract was added to the mixing dropwise. Consequently, the mixture was stirred and heated at the temperature of 70°C for 2 hours duration until a colloidal solution was formed.

During the heating process solution's color changes from green to brown indicating the presence of CuO nanoparticles.

The mixture's pH was adjusted to 12±0.02 using

(a 3505-pH meter JANEWAY).

The brown-colored solution mixture was then calcined in a 300 °C furnace for 2 hours, crushed using a ceramic mortar and pestle to produce CuO NPs, and then kept in airtight containers for further characterization and investigations.

.2.5 CHARACTERIZATION OF COPPER OXIDE NANOPARTICLES:

The UV-Vis spectrophotometer (JANEWAY 6850), with A scanning wavelength range of (200-1100nm) was used to study the optical properties.

The analysis was performed by transferring 1 ml of sample powder into a quartz cell and analyzed at room temperature using distilled water as a reference solvent. The optical band gaps were calculated by using Tauc's plot (Maku *et al.*, 2018) as shown below

$(\alpha h\nu)^{1/\gamma}=A(h\nu-Eg)$ (1)

where α is the absorption coefficient, hν photon energy, A is the absorption constant, Eg is the optical band gap energy, and γ is a factor that equals ½ for direct transmission and 2 for indirect transmission, depending on the nature of the electron transition (Mohammed, 2021).

Using an FTIR spectrophotometer (IRAffinity-1-SHAMADZO) with a wave number resolution of 1 cm^{-1} in the range(4000-500) cm^{-1} in the transmittance mode, the functional groups of the extract and nanoparticles were identified. Also, it was used to identify the bioactive chemicals accountable for copper ion reduction and capping (Gopalakrishnan *et al*., 2012; Mohamed, 2020; Renuga *et al*., 2020; Saif *et al*., 2016).

Using Cu(K) radiation (wavelength: 1.5406 Å) and operating at 40 kV and 40 mA at room temperature, an X-ray diffractometer (XRD) (ray diffraction system X-Pert Pro) revealed the crystal structure of NPs with a scanning range angles between 10 and 80 degrees. The average crystal size was calculated using the Debye-Scherrer formula. (Raj & Lawerence, 2018)

$D = \frac{k\lambda}{\beta cos\theta}$ (2) where

D is the size of the particle, k is a constant equal to 0.94, λ is the X-ray source's wavelength equal to (0.1541 nm), and β is the full width at half maximum (FWHM)(Salim, 2016).

The interplanar distance of CuO NPs for the preferred orientation peaks was measured using Bragg's law (Dowsett et al., 2021)(Humphreys, 2013) as follows:

$n\lambda=2d\sin\theta$ (3)

The dislocation density (δ) and strain (ε) were determined by Equations (4) and (5), respectively(Abdulqudos & Abdulrahman, 2022).

$\delta = \frac{1}{D^2}$ (4)

$\varepsilon = \frac{\beta \cos\theta}{4}$ (5)

Field-Emission Scanning electron microscopy (SEM-TESCAN VEGA 3) was utilized to investigate the nanoparticles' morphology. The average size of the fabricated CuO NPs was measured using FESEM along with energy-dispersive X-ray (EDX) for compositional analysis.

2.6 NPs Formation Mechanism:

The Biosynthesis of plant-mediated nanoparticles is divided into three phases: reduction, growth, and stabilization. Metal ions are recovered from their salt precursors by the interaction of plant metabolites; biomolecules that possess reduction capabilities, making this phase the most important. Nucleation of the reduced metal atoms occurs when the metal ions are reduced from their mono/divalent oxidation states to zero valent states. Further biological reduction of metal ions occurs during the growth phase when the metal atoms which have been separated begin to recombine to create metal nanoparticles. Although widespread nucleation has the potential to aggregate newly synthesized nanoparticles, changing their morphologies, the growth phase increases in the enhanced thermodynamic steadiness of nanoparticles. Nanoparticle stabilization is the last phase in the biosynthesis process. Capping the nanoparticles with plant metabolites gives them the most stable and steady morphology of nanoparticles. Nanoparticle stabilization is the last phase in the biosynthesis process. Capping the nanoparticles with plant metabolites gives them the most stable and steady morphology. Green synthesis, the formation NPs mechanism which used plants, is shown in Figure 4 (Barzinjy et al., 2020; Barzinjy & Azeez, 2020)

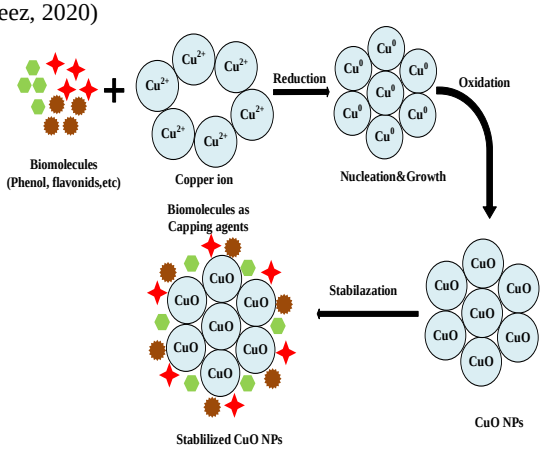

Figure (4): mechanism NPs fabrication

3. RESULTS AND DISCUSSION

3.1 Visual Observation:

The primary indication that CuO NPs were synthesized was the color change of the reaction mixture. Immediately after Ferulago angulates [Schltdl.] BOISS was added to the colorless 1 M Cu $(NO_3)_2.3H_2O$ solution, and the color of the solution began to change to pale turquoise.

The solution's color changed from pale turquoise to pine green and finally to pale yellow when it came into contact with the NaOH solution. The appearance of these color changes, which are brought on by the excitation of surface plasmon resonance in the metal oxide nanoparticles, is an indication that CuO NPs have been fabricated (Kiflom Gebremedhn *et al.*, 2019; Berra *et al.*, 2018). Also, the color change can be related to the oscillation modes of conduction electrons and incident electromagnetic radiation (Berra *et al.*,2018) which is an indication of CuO Ns formation.

In contrast, the leaf extract of Ferulago angulates [Schltdl.] BOISS and the Cu $(NO3)_2.3H2O$ solution remained unchanged in color (Figure 1 b).

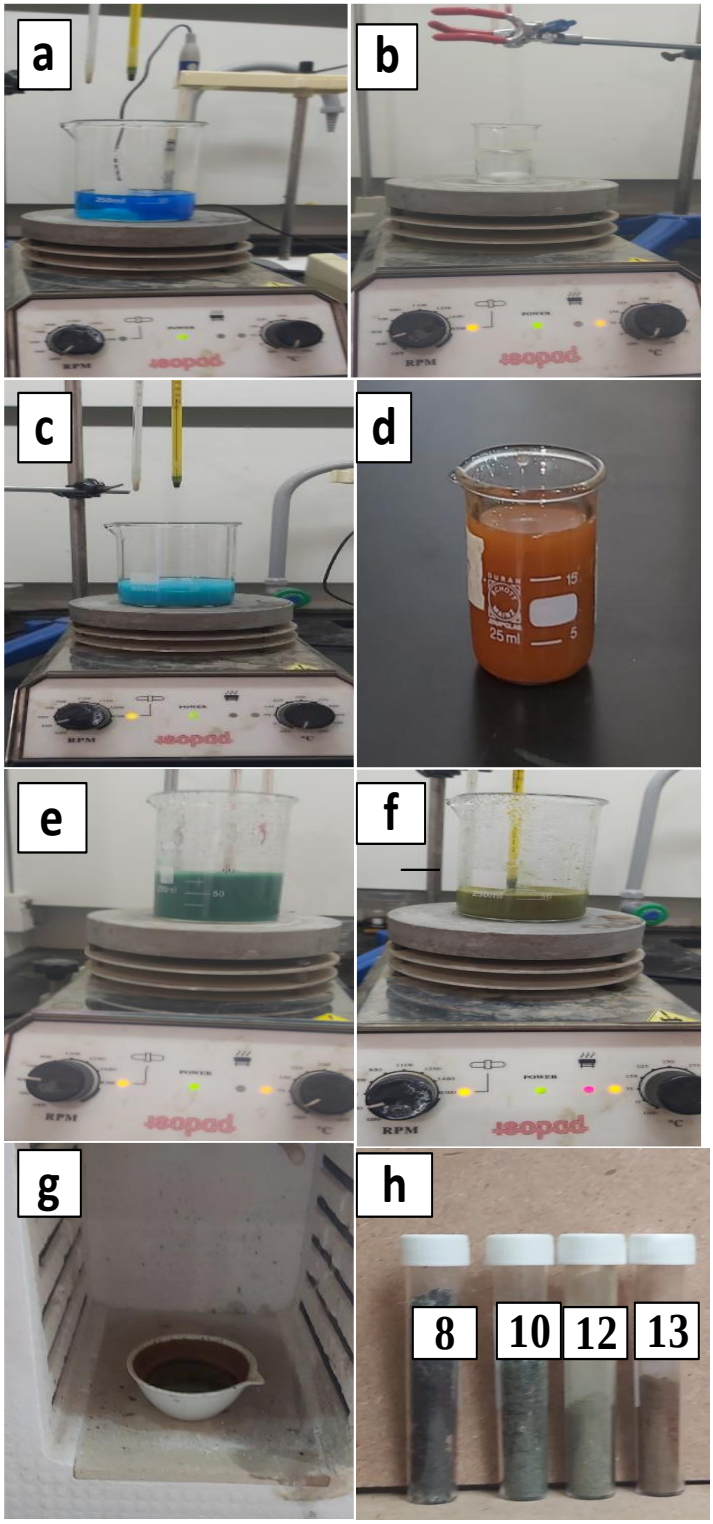

Figure (5): Steps for Copper Oxide Nanoparticles Preparation where (a) Cu $(NO_3)_2.3H_2O$, (b)NaOH, (c) Cu $(NO_3)_2.3H_2O$ and NaOH mixture, (d) Ferulago angulate [Schltdl.] BOISS Leaves Extract, (e,f) Cu$(NO_3)_2.3H_2O$, NaOH and, Ferulago angulate [Schltdl.] BOISS Leaves Extract mixture and, (g,h) CuO NPs

3.2 Phytochemical analysis of Ferulago angulate [Schltdl.] BOISS leaf extract:

Standard test methods were used to analyze the chemical components of an aqueous leaf extract of Ferulago angulate (Schltdl.) BOISS to verify the presence of active phytochemicals (Schltdl.).

Tannins, alkaloids, flavonoids, phenols, and anthocyanins were found, based on the results of the phytochemical analysis. (Table.1) (Nafeesa et al, 2017; Tyagi, 2017).

Table 1: Phytochemical analysis

Plant Metabolite	Ferulago angulate [Schltdl.] BOISS leaf extract results
Flavonoid	+
Carbohydrate	+
Alkaloid	+
Tannin	+
Saponin	+
Proteins and amino acid	+
Phenolic	+

3.3 Fourier Transform Infrared (FTIR) Analysis:

FTIR spectra were utilized to study the structure, identification, functional groups, and chemical composition of CuO nanoparticles. Spectra of the solid phase obtained by FTIR were collected between 4000 and 500 cm^{-1} and compared with the standard FTIR spectra(Gopalakrishnan *et al*., 2012; Mohamed, 2020; Renuga *et al*., 2020; Saif *et al*., 2016).

Figure (6) shows the FTIR spectra of the Ferulago angulate (Schltdl.) BOISS leaf extract, and Table 3 (provides a list of the functional groups that correspond to those spectra).

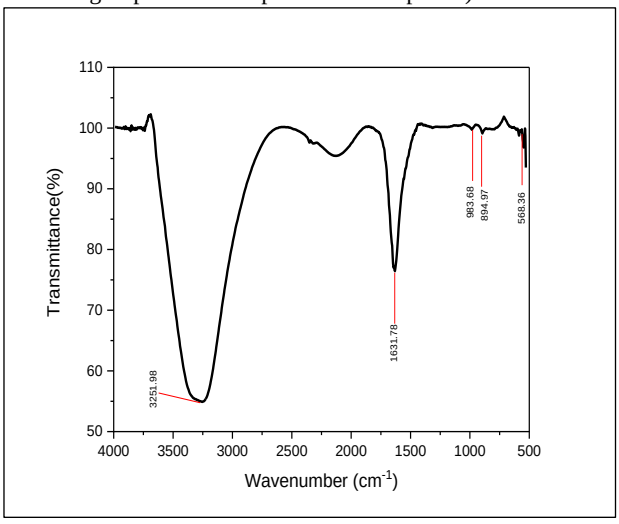

Figure (6): shows the FTIR spectrum of a leaf extract from Ferulago angulate (Schltdl.) BOISS

Table 2. The functional groups exist in the Ferulago angulate [Schltdl.] BOISS leaf extract

pH	Wavenumber (cm^{-1})	Functional Groups
8	3344.57	N-H aliphatic primary amine
	2353.15	O=C=O carbon dioxide
	1786.08	=O conjugated acid halide
	1624.06	-H amine
	1342.46	O-H phenol
	829.39	C=C alkene
	779.24	C-H Alkynes
	609.5	C-Br stretching
10	1543.05	N-O nitro compound
	1342.46	O-H phenol
	829.39	C=C alkene
	779.24	C-H Alkynes
	609.5	C-Br stretching
	568.36	Cu-O Vibrations
	532.35	Cu-O Vibrations
12	1786.08	C=O acid halide
	1342.46	O-H phenol
	829.39	C-H Alkyne
	609.5	C-Br stretching
	568.36	Cu-O Vibrations
	532.35	Cu-O Vibrations
13	3344.57	N-H primary aliphatic amine
	2434.3	N-H primary amine
	1624.06	C-Br stretching
	1342.46	O-H phenol
	829.39	C=C alkene
	779.24	C-H Alkynes
	609.5	C-Br stretching
	568.36	Cu-O Vibrations
	532.35	Cu-O Vibrations

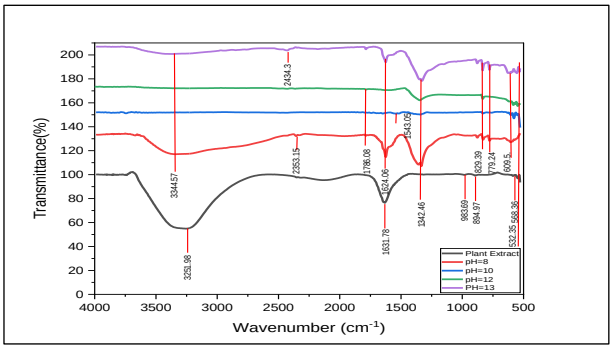

Figure (7) shows the FTIR spectrum of CuO NPs synthesized at different pH values and Table (3) lists their functional groups.

Figure (7) shows weak CuO vibration peaks at 532.35 cm^{-1}, demonstrating copper oxide nanoparticle production. After synthesizing nanoparticles, polyphenol absorption peaks at 3251.98, 1631.78, 983.69, 894.97, and 586.36 cm^{-1} indicate that Ferulago angulate [Schltdl.] BOISS extract leaves are reduces and stabilize copper oxide NPs(Berra et al., 2018).

Table 3. The functional groups exist in the CuO NPs formed at different pH

Wavenumber (cm^{-1})	Functional Group
3251.98	O-H bond of the Hydroxyl Groups (Alcohol)
1631.78	C=C conjugated Alkene
983.69	C=C Alkene
894.97	C=C Alkene
586.36	C-X Chloride

At different pH values copper oxide nanoparticles synthesis have similar functional groups but different peak intensities and frequencies. After the synthesis of CuO NPs, the Ferulago angulata [Schltdl.] BOISS extract's C=C stretching vibration observed at 1631.78 cm^{-1} reduces and shifts to 1624.06 cm^{-1}.
The O=H bending vibrations at 1342.6 cm^{-1} are correlated with the decrease in peak intensity and the increase in frequency that results from the synthesis of CuO NPs. In addition, two peaks observed at 532.35 cm^{-1} and 568.36 cm^{-1} may be ascribed to Cu-O vibrations, respectively, which agree with previous works done by other researchers (Saif *et al.*, 2016; Aminuzzaman *et al.*, 2017; Vishveshvar *et al.*, 2018; (Rehman et al., 2022).
As pH increases, aqueous extract peaks shift. Thus, biomolecules and nanoparticles of various sizes and shapes are affected by the solution's pH. This reveals that copper ions initially attach to the biomolecules' surfaces (Oza *et al.*, 2020)

3.4 STRUCTURAL ANALYSIS:

An X-ray diffractometer with XRD patterns ranging from 10° to 80° was used to confirm the crystalline phase of the produced CuO NPs.
Figure 8 shows typical XRD patterns for created copper oxide nanoparticles. The spectra reveal a monoclinic cupric oxide (CuO) and Cu_2O combination. The peaks observed at 2theta values of 32.45°, 35.75°, 35.9°, 36.45°, 39.55°, 48.6°, and 56.95°, respectively correspond to the reflection from crystal planes of (110), (002), (-111), (111), (200), (20-2), and (021) of CuO monoclinic phase. Those planes match the (CPDS Card No. 10200, 10199, ICSD Card No.01-074-1021,01-078-0428, and Card No.0011639). The peaks at 2θ ° values of 29.85°, 36.95°, and 42.85° match the planes (110), (111), and (200) of cubic Cu_2O crystalline structure (ICDD Card No. 00-003-0898).

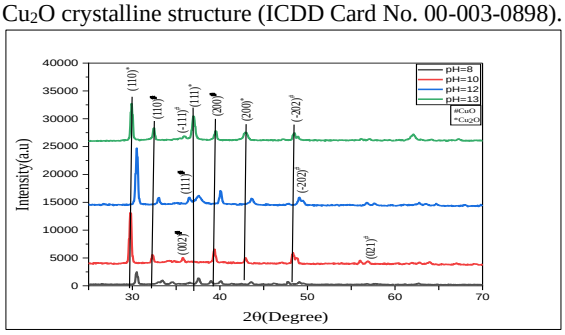

Figure (8): XRD patterns of CuO NPs for different pH.
Figure (8) shows that CuO (110) preferred orientation peak intensity increase with increasing pH values from 8 to 12.
Due to the nanocrystal structure of the CuO NPs, the position, height, and width of the diffraction peaks are all controlled by this property. The potential of grain coalescence has a role in the decrease in FWHM that occurs with an increase in pH.
The highly crystalline nature of nanoparticles is demonstrated by the sharp and narrow diffraction peaks.
The observed, standard, and calculated values of some XRD parameters for CuO thin films for the preferential orientation plane (110) using equations (2,3,4,5) are shown in Tables 4 and 5.

Table 4. The observed and standard values of XRD data for CuO NPs

pH	Observed 2θ (º)	Standard 2θ (º)	Observed d (nm)	Standard d (nm)
10	32.3	32.54	2.768	2.748
12	33.05	32.54	2.7148	2.748
13	32.45	32.54	2.759	2.748

Table 5 Calculated values of the structural parameters of CuO NPs at different PH values

Ph	2θ(º)	β	D(nm)	ε(×10^{-7})	δ(×10^{-8})
10	32.3	0.24	33.60	1.03	8.85
12	33.05	0.19	42.09	0.823	5.64
13	32.45	0.19	42.02	0.824	5.66

The X-ray diffraction technique verified the presence of nanoparticles with sizes in the ranges of (33-42) nm. However, the grain sizes estimated by Scherrer's equation were smaller than those observed in the SEM analysis (see Table 5 and Fig.8). This discrepancy can be due to the limitations of Scherrer's equation for the calculation of crystallite size. Although the CuO crystals grow larger due to annealing, recrystallization, and agglomeration of tiny crystallites, Scherrer's equation is not capable of estimating these large values (crystallite size saturation).

3.5 Morphological Analysis:

Biosynthesized CuO NPs of various surface morphologies and compositional analyses are shown in Figure (9,10) at various pH values.Figures9 and10 respectively show the SEM and EDX images of the biosynthesized CuO NPs at different pH values.

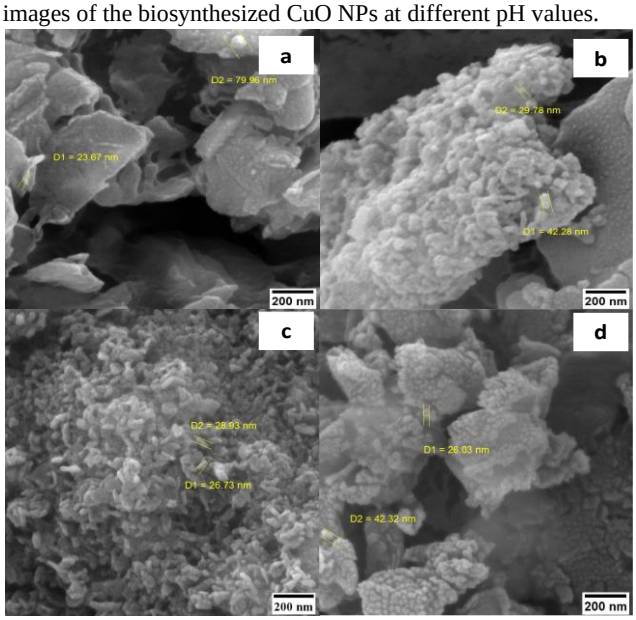

Figure (9): SEM photographs of CuO NPs for different pH of a) 8, b) 10, c) 12, and (d)13

Figure 9a (pH=8) shows the sheet-like morphology with an average sheet size in the range of 376.77 nm and is covered by tiny crystallites (NPs) of an average size of 17.64 nm. In Figure 9b (pH=10), a rough sheet-over-sheet morphology with an overall average size of 541.64 nm was observed. These sheets also are formed due to the agglomeration of tiny crystallites or nanoparticles with an average size of 22.48 nm. Figure 9c (pH

=12), shows the non-uniform distribution of agglomerated tiny crystallites or nanoparticles with an average size of 35.43nm. At pH 13 (Figure 9d), irregular grain-shaped morphology was observed. The average grain size was measured to be 486.61nm, also a closer look indicates that these grains are covered by tiny crystallites or NPs of average size in the range of 17.07nm. The morphological study indicates that the pH variation has a prominent effect on the size and shape of the fabricated CuO NPs.

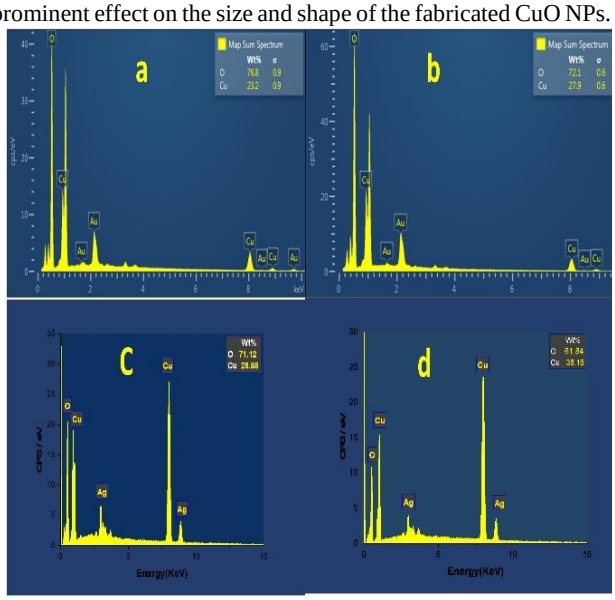

Figure (10): The elemental composition of CuO NPs using EDX analysis with different pH of (a)pH=8, (b)pH=10 (c) pH=12, and (d) pH=13.

Figures 10 (a,b,c, and d) show the EDX images of CuO biosynthesized at pH values of 8, 10, 12, and 13, respectively.

Figure 10 (a,b,c, and d) show the EDX images of CuO biosynthesized at pH values of 8,10, 12, and 13, respectively. In all EDX images, oxygen-richness (oxygen domination) was observed for the synthesized CuO samples. The EDX results also show that with increasing pH value from 8 to 12 a reduction in oxygen percentage from 76.8% to 61.8% and an increment in Cu percentage from 23.2% to 38.16 % was observed. Based on these results one should expect the energy bandgap reduction due to the reduction in the oxygen incorporation and increment in Cu incorporation which is in agreement with the the band gap values measurement shown in Section 3.6.2 (see Fig. 13 and Table 6).

Even though increasing the pH value resulted in increasing the Cu percentage which lead to band gap reduction but at the same time it also resulted in the reduction of the grain size which can cause band gap increment.

(Fishman et al., 2016);(Ben Amor et al., 2022),(Oza et al., 2020).

3.6 Optical properties of the CuO NPs:

The energy bandgap was studied using absorption spectra (Dhineshbabu & Vetumperumal, 2016).

The UV–Vis examination of pure Ferulago angulate [Schltdl.] BOISS plant extract showed a strong absorbance peak below the wavelength of 424.53nm as shown in Figure 11.

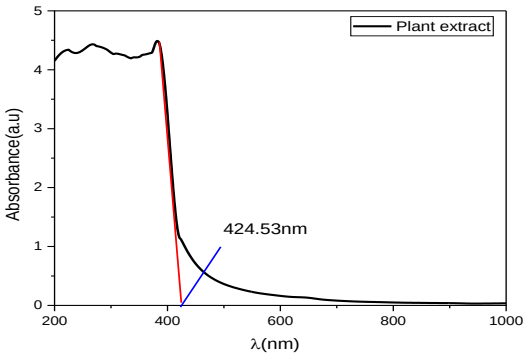

Figure (11): The absorbance spectra of pure *Ferulago* angulate [Schltdl.] BOISS plant extract.

Two methods, one visual observation of color change is used to identify the type of nanoparticles that have been targeted for synthesis from a certain plant pattern (section 3.1), and the other UV–Vis analysis can be used to identify the type of nanoparticles that have been targeted for synthesis from a certain plant.

3.6.1 Optimization of pH of the Mixture of Ferulago angulate [Schltdl.] BOISS Extract and the Precursor:

The pH value of the solution affects the bioreduction of the copper nitrate solution. The precursor and extract had pH values that were different from one another. The intensity of their peak and the redshift of their respective max values were optimized for the CuO NPs produced at various pH values (8, 10, 12, and 13). All the pH shows sharp absorption edges presenting good quality copper oxide semiconductor material as shown in Figure (12). At pH = 8, the optimum result for the synthesis of CuO NPs was shown in Figure (10).

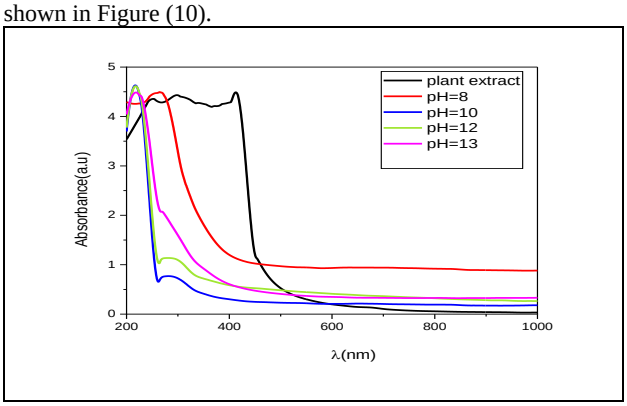

Fig(12): The absorbance spectra of CuO NPs formed at pH (a) 8, (b) 10, (c) 12, and (d) 13.

For pH 8 to 12, the plasmon resonance was stronger. When compared to pH = 8, the peak at pH = 12 was weaker but still strong. The reduction in the particle size might be responsible for the highest blue shift in the surface plasmon resonance peak, which occurred around the maximum value when pH was equal to 10(Suresh et al., 2014).

3.6.2 Energy band gap calculations:

The electronic and optical properties of materials can change when the sample size is reduced to 10 nm or less. This phenomenon is known as the quantum confinement effect. The quantum confinement effect can be observed when the size of the particle is smaller than the wavelength of the electron (Bohr radius). In NPs when quantum confinement occurs this will lead to a transition from continuous to discrete energy levels. However, when the dimensions of the material are increased (greater than Bohr radius) the transition to a discrete energy level will not occur. For this reason, the quantum confinement effect leads to bandgap widening as the particle size reduces which is

mostly observed for NPs semiconductor compounds in groups I-VI, II-V, III-V, and IV-VI (Kamarulzaman et al., 2015).

Tauc's plot technique was used to calculate the energy bandgap (Eg) of biosynthesized CuO NPs using the equation (1).

The energy bandgap for biosynthesized CuO NPS was calculated by the plotting of $(\alpha h\nu)^2$ versus photon energy ($h\nu$) for different parameters as shown in Fig.(13).

Sharp absorption h has been observed for all CuO fabricated at different pH values which represents a good quality CuO semiconductor material. It was observed that as the pH values increase the absorption edge shift toward lower energy photons.

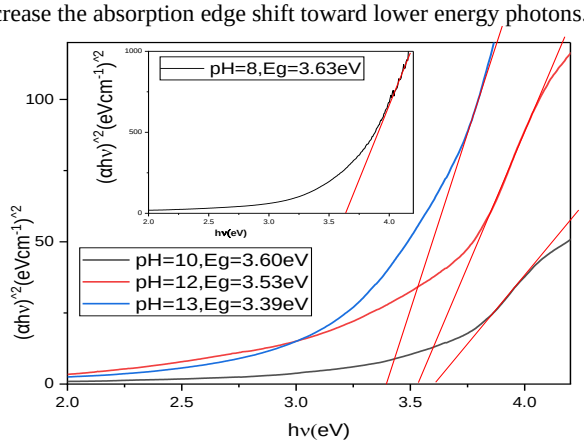

Figure. (13): Plots of $(\alpha h\upsilon)^2$ versus $h\upsilon$ for different pH values.

The calculated energy gap (Eg) using the relationship (1) is listed in Table (6)

.Table 6. The variation of Eg with pH value

pH	Eg (± 0.02) eV
8	3.63
10	3.60
12	3.53
13	3.39

From Table (6), it can be seen that the energy gap increase with increased pH.

The band gap widening can be also attributed to the larger downward shift of the VB (Kamarulzaman et al., 2015).

Many reports show that CuO has both direct and indirect bandgap depending on the synthesis method. The CuO NPs band gap values reported in this study are in agreement with those reported in the literature (Usha et al., 2015);(Tripathi et al., 2020)

3.7 The impact of pH value on the shape, size, and crystallinity... of CuO NPs

The pH which determines the level of acidity and basicity of the reaction medium has been reported to have an important impact on the shape, size, purity as well as crystallinity of the synthesized CuO NPs extracted from plant materials which are in agreement with the observations in this study (See Figure 8 and Table 5). Moreover, it has been reported that the pH variation has a significant impact on the capping and stabilizing abilities of the NPs preparation process. During the nucleation and growth stage for NPs, the local surface can be caused by protonation and deprotonation of the molecular atom as a result of pH variation (Ben Amor et al., 2022). Also, in the alkaline pH environment, the NPs are distributed and formed as a cluster in the colloidal stage preventing aggregation.

Based on XRD results, the smaller FWHM(β) and higher intensity XRD peaks were observed for the CuO NPs grown at higher pH values of 12 and 13. The smaller FWHM(β) means a higher crystallinity. Also, the effect of pH on the morphology of the CuO NPs is discussed in section (3.5).

4. CONCLUSION

In this study, the CuO NPs were successfully prepared under different pH values using Ferulago angulate leaves from the Gara mountain (Southeast of Duhok city) in the Kurdistan region.

The XRD data reveals the polycrystalline nature of the CuO NPs with an average grain size in the range of ~(33-42) nm. UV-vis study showed a sharp absorption edge indicating good quality CuO semiconductor compound fabrication with an energy gap close to those of bulk CuO. As the pH value increased, there was a corresponding reduction in the energy band gap values. FTIR shows different absorption peaks reflecting its complex structure due to biomolecules. FESEM images indicated that pH variation has a prominent effect on the shape and size of the CuO NPs which completely altered the CuO morphology (different morphology under different pH values fabrication conditions). Results obtained from EDX spectra reveal the O-richness of the prepared CuO suitable for wide band gap applications. FESEM images showed different morphology under different pH values.

Author Contributions: Conceptualization, Raghad Y. Mohammed; methodology, Raghad Y. Mohammed; software, Saniya Sadullah Omar; validation, Raghad Y. Mohammed and Saniya Sadullah Omar; formal analysis, Raghad Y. Mohammed; investigation, Raghad Y. Mohammed; resources, Raghad Y. Mohammed; data curation, Saniya Sadullah Omar; writing—original draft preparation, Saniya Sadullah Omar; writing—review and editing, Raghad Y. Mohammed; visualization, Raghad Y. Mohammed and Saniya Sadullah Omar; supervision, Raghad Y. Mohammed; project administration, Raghad Y. Mohammed; funding acquisition, University of Duhok. All authors have read and agreed to the published version of the manuscript.

Funding: This work was sponsored by the Department of Physics, College of Science, University of Duhok. This research received no external funding.

Acknowledgments: The authors would like to acknowledge the Department of Physics, College of Science, University of Duhok.

Conflicts of Interest: The authors declare no conflict of interest.

REFERENCES

Abdulqudos, A., & Abdulrahman, A. F. (2022). Biosynthesis and Characterization of ZnO Nanoparticles by using Leaf Extractionof Allium Calocephalum Wendelbow Plant. *Passer Journal of Basic and Applied Sciences*, *4*(2), 113–126. https://doi.org/10.24271/psr.2022.343112.1136

Altikatoglu, Melda and Attar, Azade and Erci, Fatih and Cristache, Corina Marilena and Isildak, I. and others. (2017). Green synthesis of copper oxide nanoparticles using Ocimum basilicum extract and their antibacterial activity. In *Fresenius Environ. Bull* (Vol. 25).

Aminuzzaman, M., Kei, L. M., & Liang, W. H. (2017). Green synthesis of copper oxide (CuO) nanoparticles using banana peel extract and their photocatalytic activities. *AIP Conference Proceedings*, *1828*. https://doi.org/10.1063/1.4979387

Azarbani, F., Saki, Z., Zareei, A., & Mohammadi, A. (2014). Phenolic contents, Antibacterial and antioxidant activities of flower, Leaf and stem extracts of ferulago angulata (schlecht) boiss. *International Journal of Pharmacy and Pharmaceutical Sciences*, *6*(10), 123–125.

Banso, A. (2009). Phytochemical and antibacterial investigation of bark extracts of Acacia nilotica. *Journal of Medicinal Plants Research*, *3*(2), 082–085.

Barzinjy, A. A., & Azeez, H. H. (2020). Green synthesis and characterization of zinc oxide nanoparticles using Eucalyptus globulus Labill. leaf extract and zinc nitrate hexahydrate salt. *SN Applied Sciences*, *2*(5), 1–14.

https://doi.org/10.1007/s42452-020-2813-1

Barzinjy, A. A., Hamad, S. M., Abdulrahman, A. F., Biro, S. J., & Ghafor, A. A. (2020). Biosynthesis, Characterization and Mechanism of Formation of ZnO Nanoparticles Using Petroselinum Crispum Leaf Extract. *Current Organic Synthesis*, *17*(7), 558–566. https://doi.org/10.2174/1570179417666200628140547

Ben Amor, M. L., Zeghdi, S., Laouini, S. E., Bouafia, A., & Meneceur, S. (2022). pH reaction effect on biosynthesis of CuO/Cu2O nanoparticles by Moringa oleifera leaves extracts for antioxidant activities. *Inorganic and Nano-Metal Chemistry*, *0*(0), 1–11. https://doi.org/10.1080/24701556.2022.2077376

Berra, D and Laouini, SE and Benhaoua, B and Ouahrani, MR and Berrani, D and Rahal, A. (2018). GREEN SYNTHESIS OF COPPER OXIDE NANOPARTICLES BY PHEONIX DACTYLIFERA L LEAVES EXTRACT. *Digest Journal of Nanomaterials and Biostructures*, *13*, 1231--1238.

Bukhari, S. I., Hamed, M. M., Al-Agamy, M. H., Gazwi, H. S. S., Radwan, H. H., & Youssif, A. M. (2021). Biosynthesis of Copper Oxide Nanoparticles Using Streptomyces MHM38 and Its Biological Applications. *Journal of Nanomaterials*, *2021*. https://doi.org/10.1155/2021/6693302

Dhineshbabu, N. R., & Vetumperumal, V. R. N. N. R. (2016). Study of structural and optical properties of cupric oxide nanoparticles. *Applied Nanoscience*, *6*(6), 933–939. https://doi.org/10.1007/s13204-015-0499-2

Doganca, S., Ulubelen, A., & Tuzlaci, E. (1991). 1-Acetylhydroquinone 4-galactoside from Ferulago aucheri. *Phytochemistry*, *30*(8), 2803–2805. https://doi.org/10.1016/0031-9422(91)85152-P

Dowsett, M., Wiesinger, R., & Adriaens, M. (2021). X-ray diffraction. *Spectroscopy, Diffraction and Tomography in Art and Heritage Science*, 161–207. https://doi.org/10.1016/B978-0-12-818860-6.00011-8

Elazab, H. A. (2018). The catalytic activity of copper oxide nanoparticles towards carbon monoxide oxidation catalysis: microwave – assisted synthesis approach. *Biointerface Research in Applied Chemistry*, *8*(3), 3278–3281.

Fishman, Z. S., Rudshteyn, B., He, Y., Liu, B., Chaudhuri, S., Askerka, M., Haller, G. L., Batista, V. S., & Pfefferle, L. D. (2016). Fundamental Role of Oxygen Stoichiometry in Controlling the Band Gap and Reactivity of Cupric Oxide Nanosheets. *Journal of the American Chemical Society*, *138*(34), 10978–10985. https://doi.org/10.1021/jacs.6b05332

Gawande, M. B., Goswami, A., Felpin, F. X., Asefa, T., Huang, X., Silva, R., Zou, X., Zboril, R., & Varma, R. S. (2016). Cu and Cu-Based Nanoparticles: Synthesis and Applications in Catalysis. *Chemical Reviews*, *116*(6), 3722–3811. https://doi.org/10.1021/acs.chemrev.5b00482

Giri, A., Pammi, S. S. S., & TVS, P. (2016). METABOLIC FINGERPRINTING OF ROOT, STEM AND LEAF EXTRACTS OF PHYLLANTHUS AMARUS. *Journal of Phytology*, *8*, 17. https://doi.org/10.19071/jp.2016.v8.2985

Golfakhrabadi, F., Ardekani, M. R. S., Saeidnia, S., Yousefbeyk, F., Jamalifar, H., Ramezani, N., Akbarzadeh, T., & Khanavi, M. (2016). Phytochemical analysis, antimicrobial, antioxidant activities and total phenols of Ferulago carduchorum in two vegetative stages (flower and fruit). *Pakistan Journal of Pharmaceutical Sciences*, *29*(2), 623–628.

Gopalakrishnan, K., Ramesh, C., Ragunathan, V., & Thamilselvan, M. (2012). Antibacterial activity of Cu2O nanoparticles on e.coli synthesized from tridax procumbens leaf extract and surface coating with polyaniline. *Digest Journal of Nanomaterials and Biostructures*, *7*(2), 833–839.

Grigore, M. E., Biscu, E. R., Holban, A. M., Gestal, M. C., & Grumezescu, A. M. (2016). Methods of synthesis, properties and biomedical applications of CuO nanoparticles. *Pharmaceuticals*, *9*(4), 1–14. https://doi.org/10.3390/ph9040075

Harborne, J. B. (1973). Methods of Plant Analysis. In *Phytochemical Methods* (pp. 1–32). https://doi.org/10.1007/978-94-009-5921-7_1

Hassan, S. E. D., Fouda, A., Radwan, A. A., Salem, S. S., Barghoth, M. G., Awad, M. A., Abdo, A. M., & El-Gamal, M. S. (2019). Endophytic actinomycetes Streptomyces spp mediated biosynthesis of copper oxide nanoparticles as a promising tool for biotechnological applications. *Journal of Biological Inorganic Chemistry*, 377–393. https://doi.org/10.1007/s00775-019-01654-5

Horti, N. C., Kamatagi, M. D., Patil, N. R., Sannaikar, M. S., & Inamdar, S. R. (2020). Synthesis and optical properties of copper oxide nanoparticles: effect of solvents. *Journal of Nanophotonics*, *14*(04), 1–9. https://doi.org/10.1117/1.jnp.14.046010

Hosseini, N., Akbari, M., Ghafarzadegan, R., Changizi Ashtiyani, S., & Shahmohammadi, R. (2012). Total phenol, antioxidant and antibacterial activity of the essential oil and extracts of Ferulago angulata ssp. angulata. 89–80 ,(43) *11* ,فصلنامه علمی پژوهشی گیاهان دارویی.

Humphreys, C. J. (2013). The significance of Braggs law in electron diffraction and microscopy, and Braggs second law. *Acta Crystallographica Section A: Foundations of Crystallography*, *69*(1), 45–50. https://doi.org/10.1107/S0108767312047587

Javidnia, A., & Khoshneviszadeh, M. (2006). Constituents of the Volatile Oil of Ferulago angulata (Schlecht.) Boiss. from Iran. *Journal of Essential Oil Research*, *18*(5), 548–550. https://doi.org/10.1080/10412905.2006.9699163

Jiménez, B., Grande, M. C., Anaya, J., Torres, P., & Grande, M. (2000). Coumarins from Ferulago capillaris and F. brachyloba. *Phytochemistry*, *53*(8), 1025–1031. https://doi.org/10.1016/S0031-9422(99)00524-5

Kamarulzaman, N., Kasim, M. F., & Rusdi, R. (2015). Band Gap Narrowing and Widening of ZnO Nanostructures and Doped Materials. *Nanoscale Research Letters*, *10*(1). https://doi.org/10.1186/s11671-015-1034-9

Kardong, D., Upadhyaya, S., & Saikia, L. R. (2013). Screening of phytochemicals, antioxidant and antibacterial activity of crude extract of Pteridium aquilinum Kuhn. *Journal of Pharmacy Research*, *6*(1), 179–182. https://doi.org/10.1016/j.jopr.2012.11.037

Karimian, H., Moghadamtousi, S. Z., Fadaeinasab, M., Golbabapour, S., Razavi, M., Hajrezaie, M., Arya, A., Abdulla, M. A., Mohan, S., Ali, H. M., & Noordin, M. I. (2014). Ferulago angulata activates intrinsic pathway of apoptosis in MCF-7 cells associated with G1 cell cycle arrest via involvement of p21/p27. *Drug Design, Development and Therapy*, *8*, 1481–1497. https://doi.org/10.2147/DDDT.S68818

Khalighi-Sigaroodi, F., Hadjiakhoondi, A., Shafiee, A., Mozaffarian, V. A., Shahverdi, A. R., & Alavi, S. H. R. (2006). Phytochemical analysis of Ferulogo Bernardii Tomk & M.Pimen. *Daru*, *14*(4), 214–221.

Kiflom Gebremedhn, Mebrahtu Hagos Kahsay, & Muluken Aklilu. (2019). Green Synthesis of CuO Nanoparticles Using Leaf Extract of Catha edulis and Its Antibacterial Activity. *Journal of Pharmacy and Pharmacology*, *7*(6).

https://doi.org/10.17265/2328-2150/2019.06.007

Kwak, K., & Kim, C. (2005). Viscosity and thermal conductivity of copper oxide nanofluid dispersed in ethylene glycol. *Korea Australia Rheology Journal*, *17*(2), 35–40.

Lakshmibai, R., Amirtham, D., & Radhika, S. (2015). Preliminary phytochemical analysis and antioxidant activities of Prosopis juliflora and Mimosa pudica leaves. *International Journal of Scientific Engineering and Technlogy Research*, *04*(30), 5766–5770.

M. Naseri, H. R. M.-E. (2013). AntioxidativeCoumarinsfromtheRootsofFerulagosubvel utina. *Asian Journal of Chemistry*, *25*(4), 1875–1878.

Mabry, J., & Moubasher, A. (1990). *Aryl esters*. *29*(3), 881–886.

Maku{\l}a, Patrycja and Pacia, Micha{\l} and Macyk, W. (2018). How to correctly determine the band gap energy of modified semiconductor photocatalysts based on UV- -Vis spectra. *The Journal of Physical Chemistry Letters*, *9*, 6814--6817.

Manasa, D. J., Chandrashekar, K. R., Madhu Kumar, D. J., Niranjana, M., & Navada, K. M. (2021). Mussaenda frondosa L. mediated facile green synthesis of Copper oxide nanoparticles – Characterization, photocatalytic and their biological investigations. *Arabian Journal of Chemistry*, *14*(6), 103184. https://doi.org/10.1016/j.arabjc.2021.103184

Melkamu, W. W., & Bitew, L. T. (2021). Green synthesis of silver nanoparticles using Hagenia abyssinica (Bruce) J.F. Gmel plant leaf extract and their antibacterial and anti-oxidant activities. *Heliyon*, *7*(11), e08459. https://doi.org/10.1016/j.heliyon.2021.e08459

Mohamed, E. A. (2020). Green synthesis of copper & copper oxide nanoparticles using the extract of seedless dates. *Heliyon*, *6*(1), e03123. https://doi.org/10.1016/j.heliyon.2019.e03123

Mohammed, R. Y. (2021). Annealing effect on the structure and optical properties of cbd-zns thin films for windscreen coating. *Materials*, *14*(22). https://doi.org/10.3390/ma14226748

Monfared, H. H., Fahimi, H., Ebrahimzade, H., Naghavi, M. R., Babaei, A., & Monfared, H. (2006). *Ar ch Ar ch of*.

Muthukumaran, S., & Gopalakrishnan, R. (2012). Structural, FTIR and photoluminescence studies of Cu doped ZnO nanopowders by co-precipitation method. *Optical Materials*, *34*(11), 1946–1953. https://doi.org/10.1016/j.optmat.2012.06.004

Nafeesa Zahid Malik1, Muhammad Riaz2, Qum Qum Noshad1, Neelum Rashid1, Q. U. A. and A. H. (2017). Morphological, phytochemical and antifungal analysis of Aloe vera L. leaf extracts. *AJAB*, 177–187.

Naik, A. V., & Sellappan, K. (2019). Physicochemical and Phytochemical Analysis of Different Plant Parts of Annona muricata L. (Annonaceae). *Pharmaceutical Methods*, *10*(2), 70–78. https://doi.org/10.5530/phm.2019.2.13

Othman, F., Sadeghian, M. S., Ebrahimi, F., & Heydari, M. (2013). A Study on Sedimentation in Sefidroud Dam by Using Depth Evaluation and Comparing the Results with USBR and FAO Methods. *International Proceedings of Chemical, Biological and Environmental Engineering*, *51*(9), 6. https://doi.org/10.7763/IPCBEE

Oza, G., Calzadilla-Avila, A. I., Reyes-Calderón, A., Anna, K. K., Ramírez-Bon, R., Tapia-Ramirez, J., & Sharma, A. (2020). pH-dependent biosynthesis of copper oxide nanoparticles using Galphimia glauca for their cytocompatibility evaluation. *Applied Nanoscience (Switzerland)*, *10*(2), 541–550. https://doi.org/10.1007/s13204-019-01159-2

Peddi, P., Ptsrk, P. R., Rani, N. U., & Tulasi, S. L. (2021). Green synthesis, characterization, antioxidant, antibacterial, and photocatalytic activity of Suaeda maritima (L.) Dumort aqueous extract-mediated copper oxide nanoparticles. *Journal of Genetic Engineering and Biotechnology*, *19*(1). https://doi.org/10.1186/s43141-021-00229-9

Raj, A., & Lawerence, R. (2018). Green synthesis and charcterization of ZnO nanoparticles from leafs extracts of Rosa indica and its antibacterial activity. *Rasayan Journal of Chemistry*, *11*(3), 1339–1348. https://doi.org/10.31788/RJC.2018.1132009

Rehman, S., Akhtar Shad, N., Munir Sajid, M., Ali, K., Javed, Y., Jamil, Y., Sajjad, M., Nawaz, A., & Kumar Sharma, S. (2022). Tuning Structural and Optical Properties of Copper Oxide Nanomaterials by Thermal Heating and Its Effect on Photocatalytic Degradation of Congo Red Dye. *Iranian Journal of Chemistry and Chemical Engineering*, *41*(5), 1549–1560. https://doi.org/10.30492/IJCCE.2021.127597.4127

Renuga, D., Jeyasundari, J., Shakthi Athithan, A. S., & Brightson Arul Jacob, Y. (2020). Synthesis and characterization of copper oxide nanoparticles using Brassica oleracea var. italic extract for its antifungal application. *Materials Research Express*, *7*(4), 45007. https://doi.org/10.1088/2053-1591/ab7b94

Saif, S., Tahir, A., Asim, T., & Chen, Y. (2016). Plant mediated green synthesis of CuO nanoparticles: Comparison of toxicity of engineered and plant mediated CuO nanoparticles towards Daphnia magna. *Nanomaterials*, *6*(11), 1–15. https://doi.org/10.3390/nano6110205

Salavati-Niasari, M., & Davar, F. (2009). Synthesis of copper and copper(I) oxide nanoparticles by thermal decomposition of a new precursor. *Materials Letters*, *63*(3–4), 441–443. https://doi.org/10.1016/j.matlet.2008.11.023

Salim, H. I. (2016). *Multilayer Solar Cells Based on CdTe Grown From Nitrate Precursor, PhD Thesis, Sheffield Hallam University, UK* (Issue March).

Shahabi, S., Hassan, Z. M., Mahdavi, M., Dezfouli, M., Rahvar, M. T., Naseri, M., & Jazani, N. H. (2007). *Ar ch ive Ar ch ive*. *11*(1), 51–59.

Shamsuddin, M., & Raja Nordin, N. (2019). Biosynthesis of copper(II) oxide nanoparticles using Murayya koeniggi aqueous leaf extract and its catalytic activity in 4-nitrophenol reduction. *Malaysian Journal of Fundamental and Applied Sciences*, *15*(2), 218–224. https://doi.org/10.11113/mjfas.v15n2.1390

Shanan, Z. J., Hadi, S. M., & Shanshool, S. K. (2018). Structural analysis of chemical and green synthesis of cuo nanoparticles and their effect on biofilm formation. *Baghdad Science Journal*, *15*(2), 211–216. https://doi.org/10.21123/BSJ.15.2.211-216

Singh, V., & Kumar, R. (2017). Study of Phytochemical Analysis and Antioxidant Activity of Allium sativum of Bundelkhand Region. *International Journal of Life-Sciences Scientific Research*, *3*(6), 1451–1458. https://doi.org/10.21276/ijlssr.2017.3.6.4

Sivaranjani, D. (2021). *Phytochemical Analysis , Antioxidant and Antidiabetic Properties of Prosopis juliflora (KaruvelamPattai) Extract*. *October*.

Sone, B. T., Diallo, A., Fuku, X. G., Gurib-Fakim, A., & Maaza, M. (2020). Biosynthesized CuO nano-platelets: Physical properties & enhanced thermal conductivity nanofluidics. *Arabian Journal of Chemistry*, *13*(1), 160–170. https://doi.org/10.1016/j.arabjc.2017.03.004

Taran, M., Safaei, M., Karimi, N., & Almasi, A. (2021). Benefits and application of nanotechnology in environmental science: an overview. *Biointerface Research in Applied Chemistry*, *11*(1), 7860–7870.

https://doi.org/10.33263/BRIAC111.78607870

Thamer, N. A., Muftin, N. Q., & Al-Rubae, S. H. N. (2018). Optimization properties and characterization of green synthesis of copper oxide nanoparticles using aqueous extract of cordia myxa L. Leaves. *Asian Journal of Chemistry*, *30*(7), 1559–1563. https://doi.org/10.14233/ajchem.2018.21242

Tripathi, A., Dixit, T., Agrawal, J., & Singh, V. (2020). Bandgap engineering in CuO nanostructures: Dual-band, broadband, and UV-C photodetectors. *Applied Physics Letters*, *116*(11). https://doi.org/10.1063/1.5128494

Tyagi, T. (2017). Phytochemical screening of active metabolites present in Eichhornia crassipes (Mart.) Solms and Pistia stratiotes (L.): Role in ethanomedicine. *Asian Journal of Pharmaceutical Education and Research*, *6*(4), 40–56.

Uma, K., Parthiban, P., & Kalpana, S. (2017). Pharmacognostical and preliminary phytochemical screening of Aavaarai Vidhai Chooranam. *Asian Journal of Pharmaceutical and Clinical Research*, *10*(10), 111–116. https://doi.org/10.22159/ajpcr.2017.v10i10.19422

Usha, V., Kalyanaraman, S., Thangavel, R., & Vettumperumal, R. (2015). Effect of catalysts on the synthesis of CuO nanoparticles: Structural and optical properties by sol-gel method. *Superlattices and Microstructures*, *86*, 203–210. https://doi.org/10.1016/j.spmi.2015.07.053

Velusamy, V., Palanisamy, S., Kokulnathan, T., Chen, S. W., Yang, T. C. K., Banks, C. E., & Pramanik, S. K. (2018). Novel electrochemical synthesis of copper oxide nanoparticles decorated graphene-β-cyclodextrin composite for trace-level detection of antibiotic drug metronidazole. *Journal of Colloid and Interface Science*, *530*, 37–45. https://doi.org/10.1016/j.jcis.2018.06.056

Vishveshvar, K., Aravind Krishnan, M. V., Haribabu, K., & Vishnuprasad, S. (2018). Green Synthesis of Copper Oxide Nanoparticles Using Ixiro coccinea Plant Leaves and its Characterization. *BioNanoScience*, *8*(2), 554–558. https://doi.org/10.1007/s12668-018-0508-5

Abdulqudos, A., & Abdulrahman, A. F. (2022). Biosynthesis and Characterization of ZnO Nanoparticles by using Leaf Extractionof Allium Calocephalum Wendelbow Plant. *Passer Journal of Basic and Applied Sciences*, *4*(2), 113–126. https://doi.org/10.24271/psr.2022.343112.1136

Altikatoglu, Melda and Attar, Azade and Erci, Fatih and Cristache, Corina Marilena and Isildak, I. and others. (2017). Green synthesis of copper oxide nanoparticles using Ocimum basilicum extract and their antibacterial activity. In *Fresenius Environ. Bull* (Vol. 25).

Aminuzzaman, M., Kei, L. M., & Liang, W. H. (2017). Green synthesis of copper oxide (CuO) nanoparticles using banana peel extract and their photocatalytic activities. *AIP Conference Proceedings*, *1828*. https://doi.org/10.1063/1.4979387

Azarbani, F., Saki, Z., Zareei, A., & Mohammadi, A. (2014). Phenolic contents, Antibacterial and antioxidant activities of flower, Leaf and stem extracts of ferulago angulata (schlecht) boiss. *International Journal of Pharmacy and Pharmaceutical Sciences*, *6*(10), 123–125.

Banso, A. (2009). Phytochemical and antibacterial investigation of bark extracts of Acacia nilotica. *Journal of Medicinal Plants Research*, *3*(2), 082–085.

Barzinjy, A. A., & Azeez, H. H. (2020). Green synthesis and characterization of zinc oxide nanoparticles using Eucalyptus globulus Labill. leaf extract and zinc nitrate hexahydrate salt. *SN Applied Sciences*, *2*(5), 1–14. https://doi.org/10.1007/s42452-020-2813-1

Barzinjy, A. A., Hamad, S. M., Abdulrahman, A. F., Biro, S. J., & Ghafor, A. A. (2020). Biosynthesis, Characterization and Mechanism of Formation of ZnO Nanoparticles Using Petroselinum Crispum Leaf Extract. *Current Organic Synthesis*, *17*(7), 558–566. https://doi.org/10.2174/1570179417666200628140547

Ben Amor, M. L., Zeghdi, S., Laouini, S. E., Bouafia, A., & Meneceur, S. (2022). pH reaction effect on biosynthesis of CuO/Cu2O nanoparticles by Moringa oleifera leaves extracts for antioxidant activities. *Inorganic and Nano-Metal Chemistry*, *0*(0), 1–11. https://doi.org/10.1080/24701556.2022.2077376

Berra, D and Laouini, SE and Benhaoua, B and Ouahrani, MR and Berrani, D and Rahal, A. (2018). GREEN SYNTHESIS OF COPPER OXIDE NANOPARTICLES BY PHEONIX DACTYLIFERA L LEAVES EXTRACT. *Digest Journal of Nanomaterials and Biostructures*, *13*, 1231--1238.

Bukhari, S. I., Hamed, M. M., Al-Agamy, M. H., Gazwi, H. S. S., Radwan, H. H., & Youssif, A. M. (2021). Biosynthesis of Copper Oxide Nanoparticles Using Streptomyces MHM38 and Its Biological Applications. *Journal of Nanomaterials*, *2021*. https://doi.org/10.1155/2021/6693302

Dhineshbabu, N. R., & Vetumperumal, V. R. N. N. R. (2016). Study of structural and optical properties of cupric oxide nanoparticles. *Applied Nanoscience*, *6*(6), 933–939. https://doi.org/10.1007/s13204-015-0499-2

Doganca, S., Ulubelen, A., & Tuzlaci, E. (1991). 1-Acetylhydroquinone 4-galactoside from Ferulago aucheri. *Phytochemistry*, *30*(8), 2803–2805. https://doi.org/10.1016/0031-9422(91)85152-P

Dowsett, M., Wiesinger, R., & Adriaens, M. (2021). X-ray diffraction. *Spectroscopy, Diffraction and Tomography in Art and Heritage Science*, 161–207. https://doi.org/10.1016/B978-0-12-818860-6.00011-8

Elazab, H. A. (2018). The catalytic activity of copper oxide nanoparticles towards carbon monoxide oxidation catalysis: microwave – assisted synthesis approach. *Biointerface Research in Applied Chemistry*, *8*(3), 3278–3281.

Fishman, Z. S., Rudshteyn, B., He, Y., Liu, B., Chaudhuri, S., Askerka, M., Haller, G. L., Batista, V. S., & Pfefferle, L. D. (2016). Fundamental Role of Oxygen Stoichiometry in Controlling the Band Gap and Reactivity of Cupric Oxide Nanosheets. *Journal of the American Chemical Society*, *138*(34), 10978–10985. https://doi.org/10.1021/jacs.6b05332

Gawande, M. B., Goswami, A., Felpin, F. X., Asefa, T., Huang, X., Silva, R., Zou, X., Zboril, R., & Varma, R. S. (2016). Cu and Cu-Based Nanoparticles: Synthesis and Applications in Catalysis. *Chemical Reviews*, *116*(6), 3722–3811. https://doi.org/10.1021/acs.chemrev.5b00482

Giri, A., Pammi, S. S. S., & TVS, P. (2016). METABOLIC FINGERPRINTING OF ROOT, STEM AND LEAF EXTRACTS OF PHYLLANTHUS AMARUS. *Journal of Phytology*, *8*, 17. https://doi.org/10.19071/jp.2016.v8.2985

Golfakhrabadi, F., Ardekani, M. R. S., Saeidnia, S., Yousefbeyk, F., Jamalifar, H., Ramezani, N., Akbarzadeh, T., & Khanavi, M. (2016). Phytochemical analysis, antimicrobial, antioxidant activities and total phenols of Ferulago carduchorum in two vegetative stages (flower and fruit). *Pakistan Journal of Pharmaceutical Sciences*, *29*(2), 623–628.

Gopalakrishnan, K., Ramesh, C., Ragunathan, V., & Thamilselvan, M. (2012). Antibacterial activity of Cu2O nanoparticles on e.coli synthesized from tridax

procumbens leaf extract and surface coating with polyaniline. *Digest Journal of Nanomaterials and Biostructures*, *7*(2), 833–839.

Grigore, M. E., Biscu, E. R., Holban, A. M., Gestal, M. C., & Grumezescu, A. M. (2016). Methods of synthesis, properties and biomedical applications of CuO nanoparticles. *Pharmaceuticals*, *9*(4), 1–14. https://doi.org/10.3390/ph9040075

Harborne, J. B. (1973). Methods of Plant Analysis. In *Phytochemical Methods* (pp. 1–32). https://doi.org/10.1007/978-94-009-5921-7_1

Hassan, S. E. D., Fouda, A., Radwan, A. A., Salem, S. S., Barghoth, M. G., Awad, M. A., Abdo, A. M., & El-Gamal, M. S. (2019). Endophytic actinomycetes Streptomyces spp mediated biosynthesis of copper oxide nanoparticles as a promising tool for biotechnological applications. *Journal of Biological Inorganic Chemistry*, 377–393. https://doi.org/10.1007/s00775-019-01654-5

Horti, N. C., Kamatagi, M. D., Patil, N. R., Sannaikar, M. S., & Inamdar, S. R. (2020). Synthesis and optical properties of copper oxide nanoparticles: effect of solvents. *Journal of Nanophotonics*, *14*(04), 1–9. https://doi.org/10.1117/1.jnp.14.046010

Hosseini, N., Akbari, M., Ghafarzadegan, R., Changizi Ashtiyani, S., & Shahmohammadi, R. (2012). Total phenol, antioxidant and antibacterial activity of the essential oil and extracts of Ferulago angulata ssp. angulata. 89–80 ,(43)*11* ,فصلنامه علمی پژوهشی گیاهان دارویی

Humphreys, C. J. (2013). The significance of Braggs law in electron diffraction and microscopy, and Braggs second law. *Acta Crystallographica Section A: Foundations of Crystallography*, *69*(1), 45–50. https://doi.org/10.1107/S0108767312047587

Javidnia, A., & Khoshneviszadeh, M. (2006). Constituents of the Volatile Oil of Ferulago angulata (Schlecht.) Boiss. from Iran. *Journal of Essential Oil Research*, *18*(5), 548–550. https://doi.org/10.1080/10412905.2006.9699163

Jiménez, B., Grande, M. C., Anaya, J., Torres, P., & Grande, M. (2000). Coumarins from Ferulago capillaris and F. brachyloba. *Phytochemistry*, *53*(8), 1025–1031. https://doi.org/10.1016/S0031-9422(99)00524-5

Kamarulzaman, N., Kasim, M. F., & Rusdi, R. (2015). Band Gap Narrowing and Widening of ZnO Nanostructures and Doped Materials. *Nanoscale Research Letters*, *10*(1). https://doi.org/10.1186/s11671-015-1034-9

Kardong, D., Upadhyaya, S., & Saikia, L. R. (2013). Screening of phytochemicals, antioxidant and antibacterial activity of crude extract of Pteridium aquilinum Kuhn. *Journal of Pharmacy Research*, *6*(1), 179–182. https://doi.org/10.1016/j.jopr.2012.11.037

Karimian, H., Moghadamtousi, S. Z., Fadaeinasab, M., Golbabapour, S., Razavi, M., Hajrezaie, M., Arya, A., Abdulla, M. A., Mohan, S., Ali, H. M., & Noordin, M. I. (2014). Ferulago angulata activates intrinsic pathway of apoptosis in MCF-7 cells associated with G1 cell cycle arrest via involvement of p21/p27. *Drug Design, Development and Therapy*, *8*, 1481–1497. https://doi.org/10.2147/DDDT.S68818

Khalighi-Sigaroodi, F., Hadjiakhoondi, A., Shafiee, A., Mozaffarian, V. A., Shahverdi, A. R., & Alavi, S. H. R. (2006). Phytochemical analysis of Ferulogo Bernardii Tomk & M.Pimen. *Daru*, *14*(4), 214–221.

Kiflom Gebremedhn, Mebrahtu Hagos Kahsay, & Muluken Aklilu. (2019). Green Synthesis of CuO Nanoparticles Using Leaf Extract of Catha edulis and Its Antibacterial Activity. *Journal of Pharmacy and Pharmacology*, *7*(6). https://doi.org/10.17265/2328-2150/2019.06.007

Kwak, K., & Kim, C. (2005). Viscosity and thermal conductivity of copper oxide nanofluid dispersed in ethylene glycol. *Korea Australia Rheology Journal*, *17*(2), 35–40.

Lakshmibai, R., Amirtham, D., & Radhika, S. (2015). Preliminary phytochemical analysis and antioxidant activities of Prosopis juliflora and Mimosa pudica leaves. *International Journal of Scientific Engineering and Technlogy Research*, *04*(30), 5766–5770.

M. Naseri, H. R. M.-E. (2013). AntioxidativeCoumarinsfromtheRootsofFerulagosubvelutina. *Asian Journal of Chemistry*, *25*(4), 1875–1878.

Mabry, J., & Moubasher, A. (1990). *Aryl esters*. *29*(3), 881–886.

Maku{\l}a, Patrycja and Pacia, Micha{\l} and Macyk, W. (2018). How to correctly determine the band gap energy of modified semiconductor photocatalysts based on UV- -Vis spectra. *The Journal of Physical Chemistry Letters*, *9*, 6814--6817.

Manasa, D. J., Chandrashekar, K. R., Madhu Kumar, D. J., Niranjana, M., & Navada, K. M. (2021). Mussaenda frondosa L. mediated facile green synthesis of Copper oxide nanoparticles – Characterization, photocatalytic and their biological investigations. *Arabian Journal of Chemistry*, *14*(6), 103184. https://doi.org/10.1016/j.arabjc.2021.103184

Melkamu, W. W., & Bitew, L. T. (2021). Green synthesis of silver nanoparticles using Hagenia abyssinica (Bruce) J.F. Gmel plant leaf extract and their antibacterial and anti-oxidant activities. *Heliyon*, *7*(11), e08459. https://doi.org/10.1016/j.heliyon.2021.e08459

Mohamed, E. A. (2020). Green synthesis of copper & copper oxide nanoparticles using the extract of seedless dates. *Heliyon*, *6*(1), e03123. https://doi.org/10.1016/j.heliyon.2019.e03123

Mohammed, R. Y. (2021). Annealing effect on the structure and optical properties of cbd-zns thin films for windscreen coating. *Materials*, *14*(22). https://doi.org/10.3390/ma14226748

Monfared, H. H., Fahimi, H., Ebrahimzade, H., Naghavi, M. R., Babaei, A., & Monfared, H. (2006). *Ar ch Ar ch of*.

Muthukumaran, S., & Gopalakrishnan, R. (2012). Structural, FTIR and photoluminescence studies of Cu doped ZnO nanopowders by co-precipitation method. *Optical Materials*, *34*(11), 1946–1953. https://doi.org/10.1016/j.optmat.2012.06.004

Nafeesa Zahid Malik1, Muhammad Riaz2, Qum Qum Noshad1, Neelum Rashid1, Q. U. A. and A. H. (2017). Morphological, phytochemical and antifungal analysis of Aloe vera L. leaf extracts. *AJAB*, 177–187.

Naik, A. V., & Sellappan, K. (2019). Physicochemical and Phytochemical Analysis of Different Plant Parts of Annona muricata L. (Annonaceae). *Pharmaceutical Methods*, *10*(2), 70–78. https://doi.org/10.5530/phm.2019.2.13

Othman, F., Sadeghian, M. S., Ebrahimi, F., & Heydari, M. (2013). A Study on Sedimentation in Sefidroud Dam by Using Depth Evaluation and Comparing the Results with USBR and FAO Methods. *International Proceedings of Chemical, Biological and Environmental Engineering*, *51*(9), 6. https://doi.org/10.7763/IPCBEE

Oza, G., Calzadilla-Avila, A. I., Reyes-Calderón, A., Anna, K. K., Ramírez-Bon, R., Tapia-Ramirez, J., & Sharma, A. (2020). pH-dependent biosynthesis of copper oxide nanoparticles using Galphimia glauca for their cytocompatibility evaluation. *Applied Nanoscience (Switzerland)*, *10*(2), 541–550. https://doi.org/10.1007/s13204-019-01159-2

Peddi, P., Ptsrk, P. R., Rani, N. U., & Tulasi, S. L. (2021). Green synthesis, characterization, antioxidant, antibacterial, and photocatalytic activity of Suaeda maritima (L.)

Dumort aqueous extract-mediated copper oxide nanoparticles. *Journal of Genetic Engineering and Biotechnology*, *19*(1). https://doi.org/10.1186/s43141-021-00229-9

Raj, A., & Lawerence, R. (2018). Green synthesis and charcterization of ZnO nanoparticles from leafs extracts of Rosa indica and its antibacterial activity. *Rasayan Journal of Chemistry*, *11*(3), 1339–1348. https://doi.org/10.31788/RJC.2018.1132009

Rehman, S., Akhtar Shad, N., Munir Sajid, M., Ali, K., Javed, Y., Jamil, Y., Sajjad, M., Nawaz, A., & Kumar Sharma, S. (2022). Tuning Structural and Optical Properties of Copper Oxide Nanomaterials by Thermal Heating and Its Effect on Photocatalytic Degradation of Congo Red Dye. *Iranian Journal of Chemistry and Chemical Engineering*, *41*(5), 1549–1560. https://doi.org/10.30492/IJCCE.2021.127597.4127

Renuga, D., Jeyasundari, J., Shakthi Athithan, A. S., & Brightson Arul Jacob, Y. (2020). Synthesis and characterization of copper oxide nanoparticles using Brassica oleracea var. italic extract for its antifungal application. *Materials Research Express*, *7*(4), 45007. https://doi.org/10.1088/2053-1591/ab7b94

Saif, S., Tahir, A., Asim, T., & Chen, Y. (2016). Plant mediated green synthesis of CuO nanoparticles: Comparison of toxicity of engineered and plant mediated CuO nanoparticles towards Daphnia magna. *Nanomaterials*, *6*(11), 1–15. https://doi.org/10.3390/nano6110205

Salavati-Niasari, M., & Davar, F. (2009). Synthesis of copper and copper(I) oxide nanoparticles by thermal decomposition of a new precursor. *Materials Letters*, *63*(3–4), 441–443. https://doi.org/10.1016/j.matlet.2008.11.023

Salim, H. I. (2016). *Multilayer Solar Cells Based on CdTe Grown From Nitrate Precursor*, *PhD Thesis*, *Sheffield Hallam University*, *UK* (Issue March).

Shahabi, S., Hassan, Z. M., Mahdavi, M., Dezfouli, M., Rahvar, M. T., Naseri, M., & Jazani, N. H. (2007). *Ar ch ive Ar ch ive*. *11*(1), 51–59.

Shamsuddin, M., & Raja Nordin, N. (2019). Biosynthesis of copper(II) oxide nanoparticles using Murayya koeniggi aqueous leaf extract and its catalytic activity in 4-nitrophenol reduction. *Malaysian Journal of Fundamental and Applied Sciences*, *15*(2), 218–224. https://doi.org/10.11113/mjfas.v15n2.1390

Shanan, Z. J., Hadi, S. M., & Shanshool, S. K. (2018). Structural analysis of chemical and green synthesis of cuo nanoparticles and their effect on biofilm formation. *Baghdad Science Journal*, *15*(2), 211–216. https://doi.org/10.21123/BSJ.15.2.211-216

Singh, V., & Kumar, R. (2017). Study of Phytochemical Analysis and Antioxidant Activity of Allium sativum of Bundelkhand Region. *International Journal of Life-Sciences Scientific Research*, *3*(6), 1451–1458. https://doi.org/10.21276/ijlssr.2017.3.6.4

Sivaranjani, D. (2021). *Phytochemical Analysis , Antioxidant and Antidiabetic Properties of Prosopis juliflora (KaruvelamPattai) Extract*. *October*.

Sone, B. T., Diallo, A., Fuku, X. G., Gurib-Fakim, A., & Maaza, M. (2020). Biosynthesized CuO nano-platelets: Physical properties & enhanced thermal conductivity nanofluidics. *Arabian Journal of Chemistry*, *13*(1), 160–170. https://doi.org/10.1016/j.arabjc.2017.03.004

Taran, M., Safaei, M., Karimi, N., & Almasi, A. (2021). Benefits and application of nanotechnology in environmental science: an overview. *Biointerface Research in Applied Chemistry*, *11*(1), 7860–7870. https://doi.org/10.33263/BRIAC111.78607870

Thamer, N. A., Muftin, N. Q., & Al-Rubae, S. H. N. (2018). Optimization properties and characterization of green synthesis of copper oxide nanoparticles using aqueous extract of cordia myxa L. Leaves. *Asian Journal of Chemistry*, *30*(7), 1559–1563. https://doi.org/10.14233/ajchem.2018.21242

Tripathi, A., Dixit, T., Agrawal, J., & Singh, V. (2020). Bandgap engineering in CuO nanostructures: Dual-band, broadband, and UV-C photodetectors. *Applied Physics Letters*, *116*(11). https://doi.org/10.1063/1.5128494

Tyagi, T. (2017). Phytochemical screening of active metabolites present in Eichhornia crassipes (Mart.) Solms and Pistia stratiotes (L.): Role in ethanomedicine. *Asian Journal of Pharmaceutical Education and Research*, *6*(4), 40–56.

Uma, K., Parthiban, P., & Kalpana, S. (2017). Pharmacognostical and preliminary phytochemical screening of Aavaarai Vidhai Chooranam. *Asian Journal of Pharmaceutical and Clinical Research*, *10*(10), 111–116. https://doi.org/10.22159/ajpcr.2017.v10i10.19422

Usha, V., Kalyanaraman, S., Thangavel, R., & Vettumperumal, R. (2015). Effect of catalysts on the synthesis of CuO nanoparticles: Structural and optical properties by sol-gel method. *Superlattices and Microstructures*, *86*, 203–210. https://doi.org/10.1016/j.spmi.2015.07.053

Velusamy, V., Palanisamy, S., Kokulnathan, T., Chen, S. W., Yang, T. C. K., Banks, C. E., & Pramanik, S. K. (2018). Novel electrochemical synthesis of copper oxide nanoparticles decorated graphene-β-cyclodextrin composite for trace-level detection of antibiotic drug metronidazole. *Journal of Colloid and Interface Science*, *530*, 37–45. https://doi.org/10.1016/j.jcis.2018.06.056

Vishveshvar, K., Aravind Krishnan, M. V., Haribabu, K., & Vishnuprasad, S. (2018). Green Synthesis of Copper Oxide Nanoparticles Using Ixiro coccinea Plant Leaves and its Characterization. *BioNanoScience*, *8*(2), 554–558. https://doi.org/10.1007/s12668-018-0508-5